Check for updates

Plasma Processes and Polymers

PLASMA PROCESSES AND POLYMERS

REVIEW OPEN ACCESS

"Production and Chemical Composition of Plasma Activated Water: A Systematic Review and Meta-Analysis"

Roberto Montalbetti[1] | Zdenko Machala[2] | Matteo Gherardi[1,3] | Romolo Laurita[1,4]

[1]Department of Industrial Engineering, Alma Mater Studiorum—University of Bologna, Bologna, Italy | [2]Division of Environmental Physics, Faculty of Mathematics, Physics and Informatics, Comenius University Bratislava, Bratislava, Slovakia | [3]Interdepartmental Centre for Industrial Research Advanced Mechanical Engineering Applications and Materials Technology, Alma Mater Studiorum—University of Bologna, Bologna, Italy | [4]Interdepartmental Centre for Industrial Research Health Sciences and Technologies, Alma Mater Studiorum—University of Bologna, Bologna, Italy

Correspondence: Romolo Laurita (romolo.laurita@unibo.it)

Received: 17 October 2024 | **Revised:** 4 December 2024 | **Accepted:** 6 December 2024

Funding: This work was funded by the EU NextGenerationEU through the Recovery and Resilience Plan for Slovakia under Project No. 09I03-03-V03-00033 EnvAdwice. This work was funded by the EU NextGenerationEU through the Recovery and Resilience Plan for Italy under the project "PAAFOOD Plasma activated aerosol for the preservation and decontamination of fresh and minimally processed plant foods", No. 2022W43KHF_002 – CUP J53D23010480001.

Keywords: CAP sources | cold atmospheric plasma (CAP) | PAW chemistry | plasma activated water (PAW) | reactive oxygen and nitrogen species (RONS)

ABSTRACT

The physio-chemical interplay between cold atmospheric plasma (CAP) and water confers unique chemical and biological properties to the liquid, producing plasma-activated water (PAW). This review systematically examines various methodologies for PAW production, focusing on the effects of process parameters on reactive oxygen and nitrogen species (RONS) concentration and pH levels in PAW. It presents detailed analyses of CAP sources, working gases, and treatment conditions, showcasing their impact on PAW processes. The extracted data are reprocessed to derive parameters such as mean energy density and RONS production efficiency. Specific plasma-water configurations exhibit notably higher production rates, indicating promising opportunities for advancing PAW generation techniques and enhancing its applicability in various fields.

1 | Introduction

The production and use of plasma-activated water (PAW) is a pivotal topic in plasma science and technology. The interaction between cold atmospheric plasma (CAP) and water modifies the liquid chemical properties through the production of reactive oxygen and nitrogen species (RONS) [1–9]. Even if the mechanisms behind the RONS production in PAW involve complex interactions between plasma and water, leading to the formation of both short-lived and long-lived reactive species, the scientific community generally classify dissolved RONS into two macro groups: long-lived species such as hydrogen peroxide (H_2O_2), nitrites (NO_2^-), nitrates (NO_3^-), ozone (O_3), and short-lived species such as hydroxyl radicals ($OH\cdot$), nitric oxide (NO), superoxide (O_2^-), and peroxynitrous acid (ONOOH). The mechanisms of their formation, chemical reactions, and transport can be found in detail in [1, 10–13]. The RONS endow PAW with unique biological properties [14–17], making it efficacious not only in medical treatments such as wound healing and cancer treatment [18–27], but also in agriculture processes, from seed germination to crop protection [28–35]. Additionally, PAW is effective in food processing, significantly enhancing food safety and extending product shelf life [36–43]. Moreover, scientific literature describes the use of PAW in materials processing, materials synthesis, and analytical chemistry [44–49]. The growing interest in PAW has propelled the innovation of new CAP-water processes capable of treating large volumes producing high concentrations of

This is an open access article under the terms of the Creative Commons Attribution-NonCommercial License, which permits use, distribution and reproduction in any medium, provided the original work is properly cited and is not used for commercial purposes.

© 2024 The Author(s). *Plasma Processes and Polymers* published by Wiley-VCH GmbH.

dissolved RONS. Each process parameter of PAW production, including CAP sources (Figure 1), working gas, treated liquid and volume, treatment time, and type of the power supply, specifically affects the treatment outcomes, such as discharge power, RONS concentrations, and pH values. Despite the growing interest of the scientific community, several facets related to PAW still necessitate more comprehensive studies. The chemical–physical interplay between plasma and water and how process parameters affect the pH level and concentration of dissolved RONS still require deeper investigation. This systematic review aims to provide an overview of the different CAP sources above liquid and process parameters reported in the literature to produce PAW and to investigate how the process parameters influence the induced chemistry in liquid. The meta-analysis focuses on the mean energy density of the plasma-water treatment [kWh/L] and the RONS production efficiency [mol/kWh].

2 | Methodology

2.1 | Review Strategy

This report was prepared following the PRISMA 2020 checklist and the guidelines outlined in the PRISMA statement include explanations and elaborations [50].

The identification process (Figure 2) for relevant papers begins with searches in the online Scopus and Web of Science (WOS) databases. The period starts at the beginning of 2017 and ends at the end of 2023; all papers published before or after this period were not considered. The selected keywords were "plasma-activated water" OR "plasma activated water" OR "plasma-treated water" OR "plasma treated water" OR "Plasma-functionalized water" OR "Plasma functionalized water." The search included papers and reviews, but the latter are not analyzed in this study.

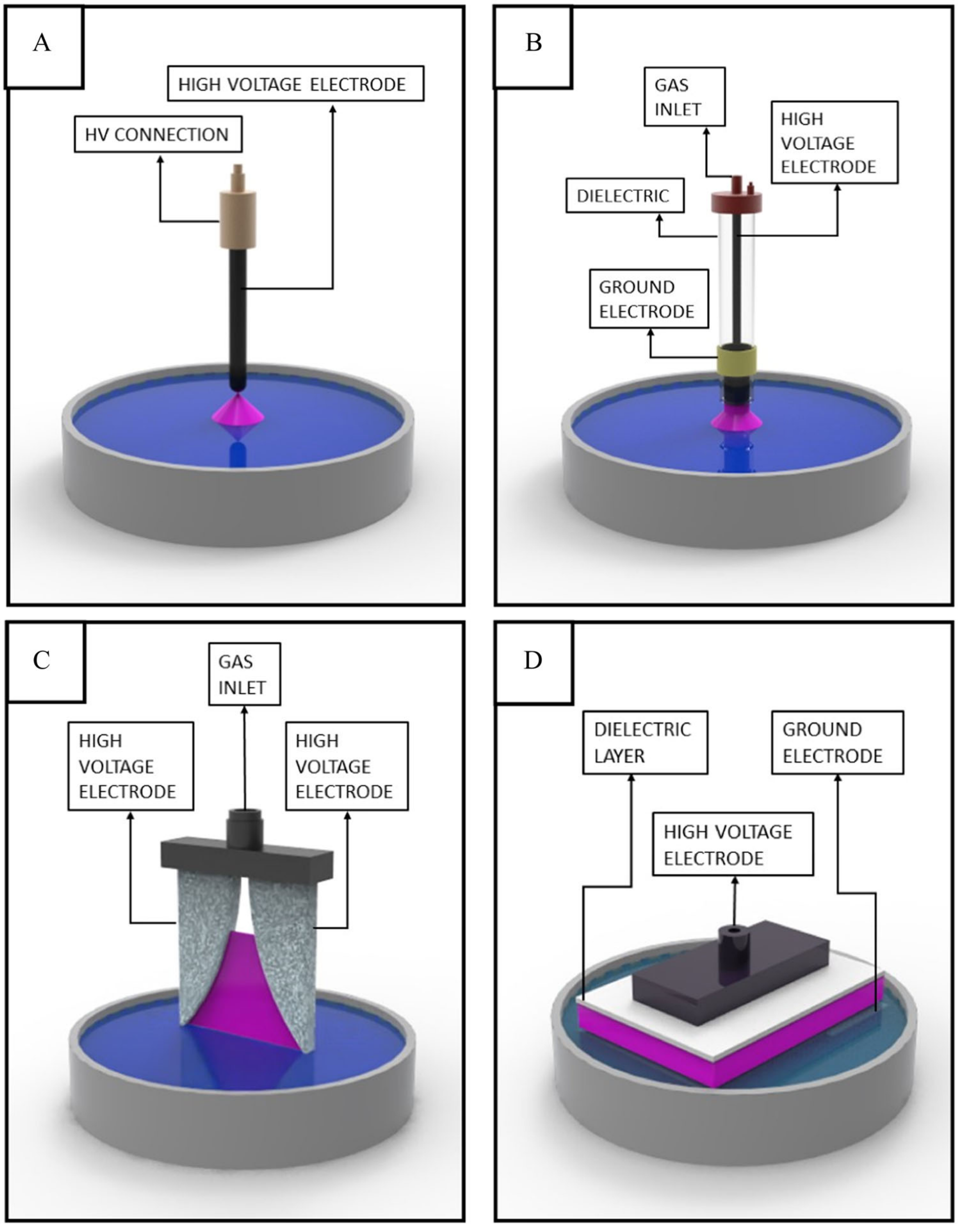

FIGURE 1 | Plasma-source for PAW treatment. (A): Corona source. (B): Plasma-jet source. (C): Gliding arc source. (D): Dielectric barrier discharge source.

16128869, 0, Downloaded from https://onlinelibrary.wiley.com/doi/10.1002/ppap.202400249 by Cochrane Slovakia, Wiley Online Library on [30/12/2024]. See the Terms and Conditions (https://onlinelibrary.wiley.com/terms-and-conditions) on Wiley Online Library for rules of use; OA articles are governed by the applicable Creative Commons License

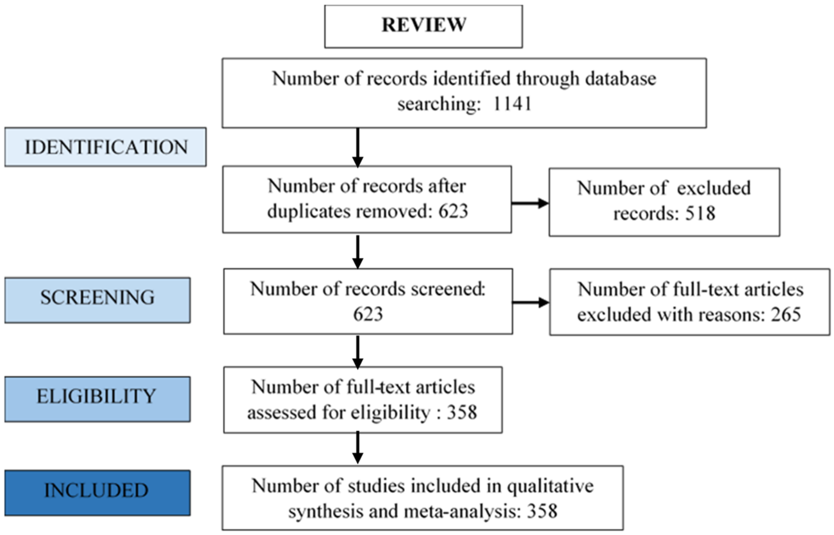

FIGURE 2 | Review strategy summary.

2.2 | Inclusion and Exclusion Criteria

Papers included in the analysis must fulfill the following specific criteria:

- The record must report PAW treatment process parameters, including treated water, working gas and flow rate, CAP source, applied voltage, frequency, current, and power supply.
- The record must contain at least two data related to: treated water and volume, working gas and flow rate, CAP source, and treatment time.
- The record must present at least two of the following results: H_2O_2 concentration, NO_2^- concentration, NO_3^- concentration, pH, and power discharge.

All records that did not meet the criteria were discarded. In addition, in the case of papers reporting more than one PAW treatment, only one was selected according to the following inclusion criteria:

- If the record reports multiple experiments based on the following criteria: working gas and gas flow rate, treatment time, and discharge power, the experiment resulting in the highest concentrations of RONS was selected.
- If the record reports multiple experiments based on the treated liquid, the experiment with tap water treatment was selected.
- If the record reports a variation of two or more of the previously mentioned experiment variables, the experiment involving air or tap water was selected (with a bias toward those with the highest concentrations of RONS).

CAP sources are classified as follows:

- Corona discharge: utilizes sharp high voltage electrodes [51]. This includes variants such as corona multi-pin, corona pin-to-plate, streamers and streamer-to-spark transition discharges [13, 52].
- DBD (Dielectric barrier discharge): involves BDa high voltage and a grounded electrode with at least one dielectric layer in the interelectrode gap [53].
- Plasma jet: features a high voltage wire electrode placed inside a dielectric tube with a working gas flowing through it [54].
- sDBD (surface Dielectric Barrier discharge): comprises a high voltage electrode positioned on a dielectric surface with a corresponding grounded electrode on the reverse side of the dielectric material [55].
- Gliding arc: composed of two tilted electrodes, with or without dielectric material, and a working gas flowing through the electrodes [56].

Microsoft Excel is used to create a database to assess the meta-analysis. Upon completing the Inclusion process, about 4000 data were processed for meta-analysis.

3 | Results

3.1 | Literature Overview

The geographical and temporal distribution of the screened papers were analyzed. Figure 3 describes the number of papers and reviews published between 2017 and 2023. Despite the moderate initial number of publications in the first 2 years, there is a remarkable increase between 2020 and 2023. This underlined the extending prominence of PAW processes and led to the global expansion of PAW-related papers (as illustrated in Figure 4). The Asian continent is predominant (total 48%; China 22%, India 5%, and Japan 3%). Europe emerges as the second most significant region in terms of contributors (total 29%; Italy 6%, Slovakia 5%, and Germany 3%), followed by America (total 12%; USA 8% and Canada 3%), and Oceania (total 10%; 6% Australia).

16128869, 0, Downloaded from https://onlinelibrary.wiley.com/doi/10.1002/ppap.202400249 by Cochrane Slovakia, Wiley Online Library on [30/12/2024]. See the Terms and Conditions (https://onlinelibrary.wiley.com/terms-and-conditions) on Wiley Online Library for rules of use; OA articles are governed by the applicable Creative Commons License

3.2 | Methods for the Production of PAW

The following charts (Figures 5–7) report the annual number of papers published between 2017 and 2023, classified by the CAP source, working gas, and typology of the power supply used for PAW production.

Figure 5 depicts the CAP sources most widely used over the years. The most utilized is the plasma jet (47%), succeeded by the DBD at 24% and the corona discharge at 16%. CAP sources such as gliding arc and sDBD each contribute 7%.

Figure 6 reports the most employed working gas for PAW production, with air being prevalent (65%), despite biases induced by the inclusion criteria influencing this preference. Other frequently used gases are Ar (14%), N_2 (6%), and

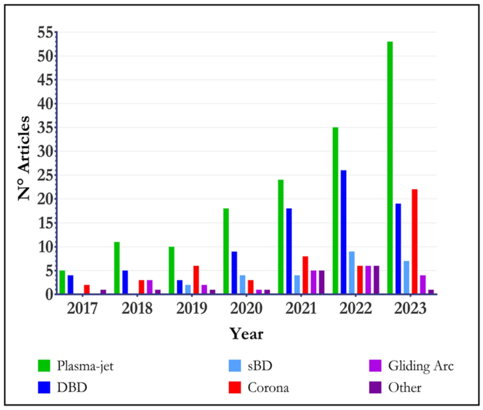

FIGURE 5 | Yearly distribution of CAP sources used for PAW production.

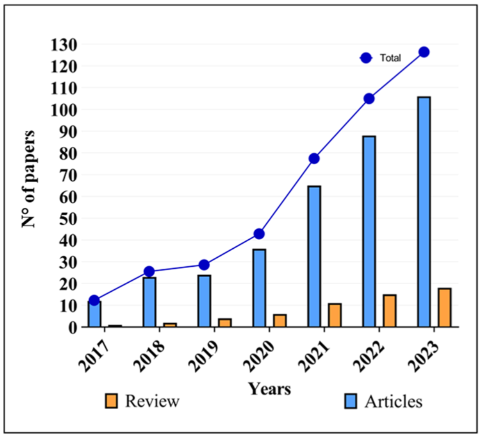

FIGURE 3 | Yearly distribution of the screened papers.

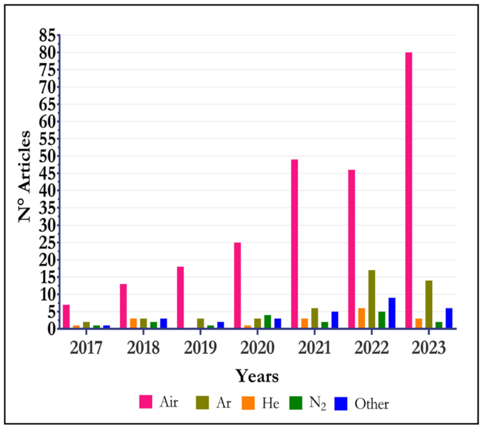

FIGURE 6 | Yearly distribution of the working gas used for PAW production.

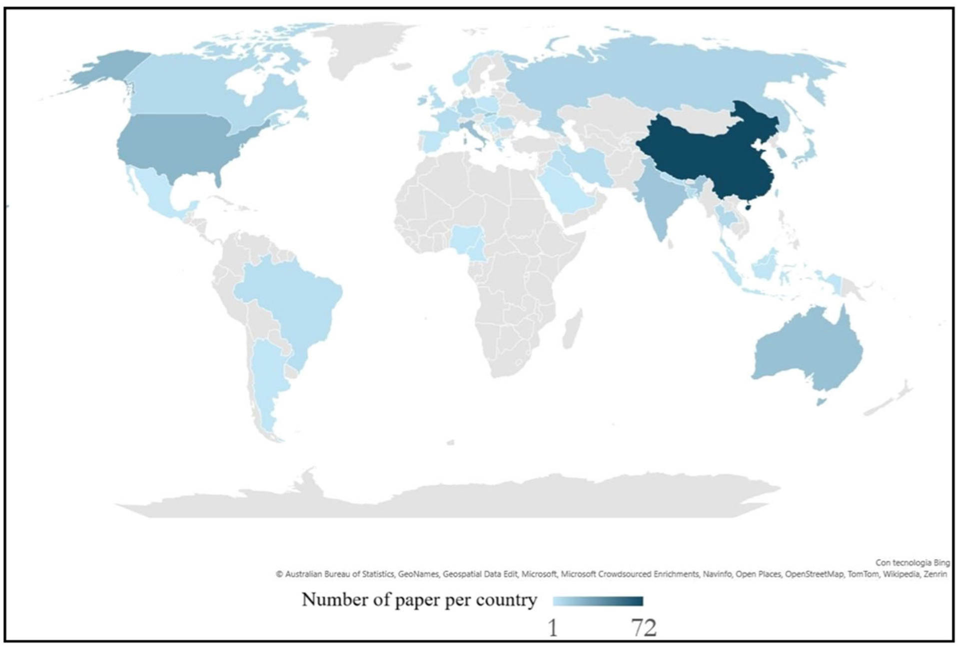

FIGURE 4 | Geographic distribution of the screened papers.

16128869, 0, Downloaded from https://onlinelibrary.wiley.com/doi/10.1002/ppap.202400249 by Cochrane Slovakia, Wiley Online Library on [30/12/2024]. See the Terms and Conditions (https://onlinelibrary.wiley.com/terms-and-conditions) on Wiley Online Library for rules of use; OA articles are governed by the applicable Creative Commons License

He (5%). Mixtures of different gases (e.g., $Ar + O_2$, $O_2 + N_2$, He + air) are used and were classified as "Other" (6%).

Figure 7 presents the typologies of power supplies used for CAP generation. Sinusoidal voltage (in kHz frequency range) and microsecond or nanosecond pulsed voltages are the most commonly utilized waveforms generated by power supplies, accounting for 44% and 39%, respectively. Other power supplies produce waveforms such as microwave (4%), bi-polar (5%), and radiofrequency (7%).

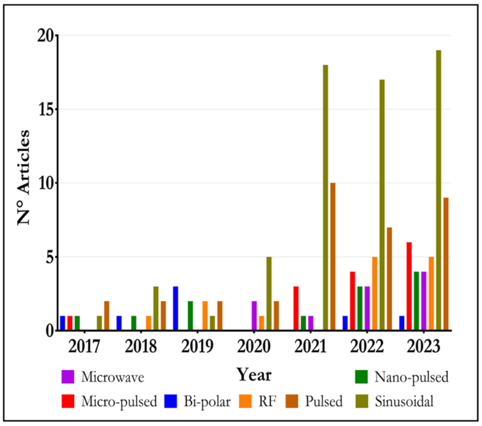

FIGURE 7 | Yearly distribution of the used waveform generated by power supply used for PAW production.

3.3 | Influence of the Type of Water and Plasma Source on RONS Concentration

PAW production involves various types of water derived through different chemical and physical procedures such as distillation, deionization, tap water production, and reverse osmosis. Deionized water is the most commonly used, accounting for 40% of the total, followed by distilled water 34%. Recent years exhibit an increase in tap water use, constituting 10% of the liquids used in PAW processes. Other types of treated water, such as ultrapure water (7%) and reverse osmosis water (2%), are also employed in PAW production. Figures 8–10 illustrate the concentrations of the most typical long-lived RONS (H_2O_2, NO_2^-, NO_3^-) produced in PAW by treating different types of water using various CAP sources. To emphasize the difference between buffered and non-buffered liquids, water types are classified as pure (including distilled water, de-ionized water, ultrapure water, reverse osmosis water) and tap water. The plasma sources depicted are plasma jets, DBDs, and corona discharges (excluding gliding arc due to a lack of data). In Figure 11, the median of the concentration of long-lived RONS is reported. The analysis of H_2O_2 concentrations (Figure 11) indicates that plasma jets can produce the highest median concentrations either in pure or tap water, succeeded by DBDs and corona discharges. Pure water results in significantly higher H_2O_2 median concentrations than tap water, regardless the CAP source utilized within the treatment. Regarding NO_2^- concentrations (Figure 11), plasma jets again provide the highest median concentrations, followed by DBDs and corona discharges. The reported median of NO_2^- concentrations produced using plasma jet and DBD are

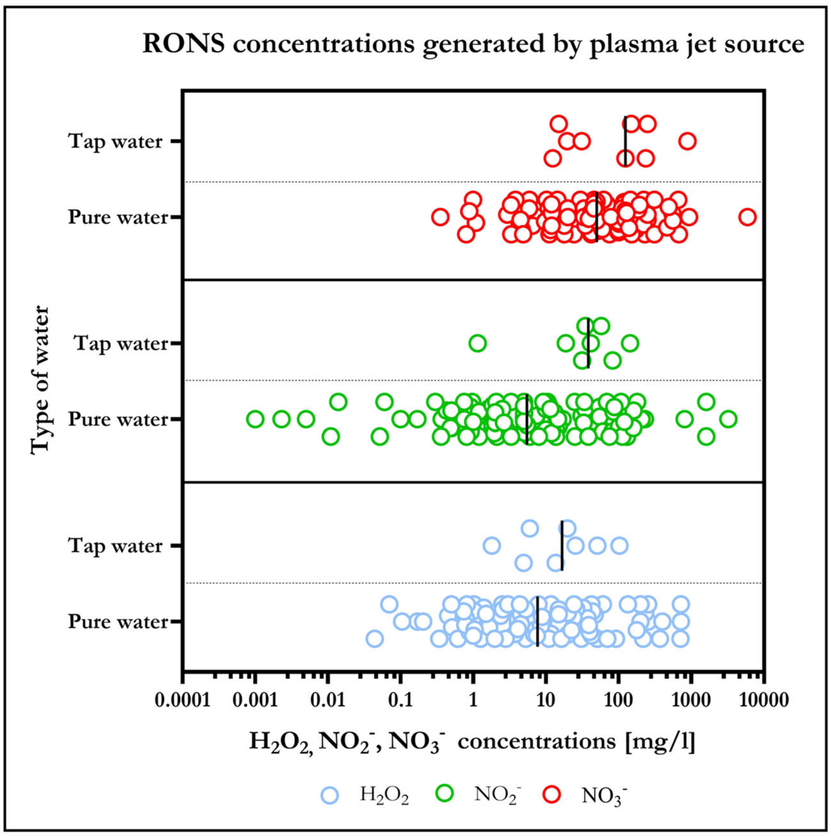

FIGURE 8 | Influence of the type of water on concentrations of RONS (H_2O_2, NO_2^-, NO_3^-), produced with plasma jet CAP source. The black line represents the median.

16128869, 0, Downloaded from https://onlinelibrary.wiley.com/doi/10.1002/ppap.202400249 by Cochrane Slovakia, Wiley Online Library on [30/12/2024]. See the Terms and Conditions (https://onlinelibrary.wiley.com/terms-and-conditions) on Wiley Online Library for rules of use; OA articles are governed by the applicable Creative Commons License

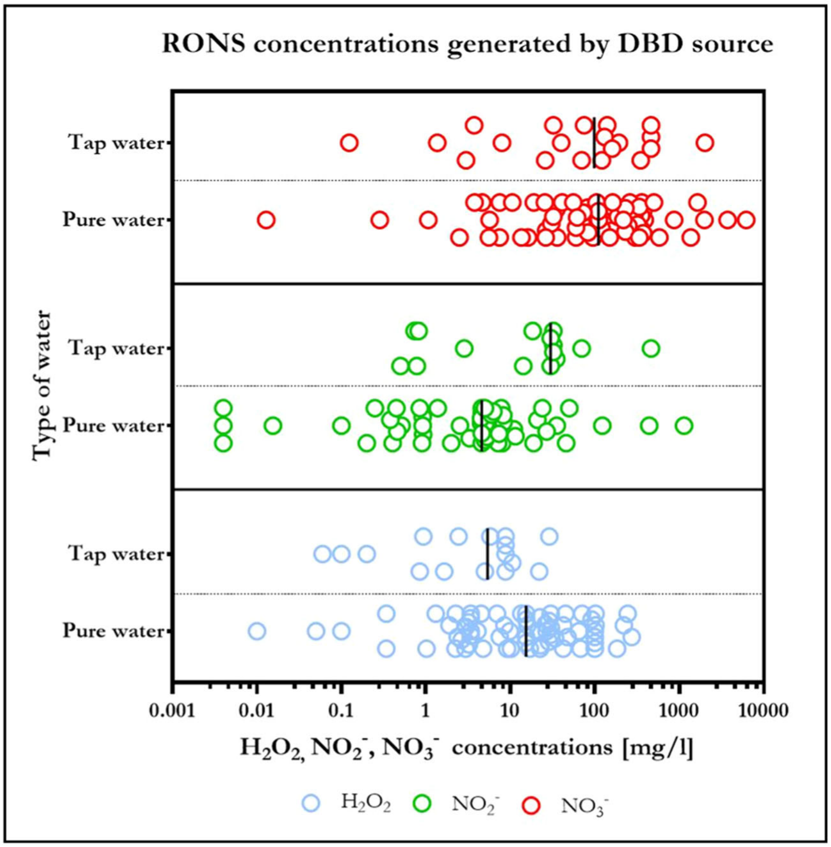

FIGURE 9 | Influence of the type of water on concentrations of RONS (H_2O_2, NO_2^-, NO_3^-), produced with DBD CAP source. The black line represents the median.

higher when treating tap water than pure one. In contrast, corona discharge exhibits almost the same median value, indecently from the used water. The data related to NO_3^- concentrations (Figure 11) confirm the previously observed trend, wherein the plasma jets have the highest median NO_3^- concentrations. In this instance, the corona discharge and plasma jet sources produce higher median concentrations when treating tap water than pure water. Notably, nitrate concentrations in tap water can be affected by the presence of nitrates in the untreated water itself.

3.4 | Influence of Type of Water, Volume, and Plasma Sources on RONS Concentration

Figures 12–14 illustrate the correlation between the volume (in liters) and concentrations (mg/L) of H_2O_2, NO_2^-, and NO_3^- in pure and tap water treated using CAP sources. Figure 12A depicts the H_2O_2 concentration distribution in pure water. Few papers report a treated volume higher than 0.5 L; only those under 0.25 L reach the highest concentrations (200 mg/L). Conversely, in tap water (Figure 12B), H_2O_2 concentrations are markedly lower, with maximum values of 28 mg/L.

Figure 13A displays NO_2^- concentrations; almost all the papers report treated volumes lower than 0.5 L, and exclusively, treated volumes below 0.4 L report the highest concentrations (230 mg/L). In this instance, the plasma jet and gliding arc yield the highest concentrations. NO_2^- concentrations in tap water (Figure 13B) are lower than in pure water, with many papers reporting concentrations below 50 mg/L.

NO_3^- concentrations in pure water (Figure 14A) reveal a wide distribution across different CAP sources. As reported for NO_2^- and H_2O_2, also in this case, the major part of the paper reports treated volumes below 0.5 L, and those under 0.25 L secure the highest concentrations (500 mg/L) of nitrate, achieved with plasma jet and gliding arc. Figure 14B depicts NO_3^- concentrations in tap water, showing similar maximum values to those in pure water. These graphs demonstrate the differential impact of various cold plasma sources on generating RONS in pure versus tap water, highlighting the influence of the treated volume on the concentration of different RONS.

3.5 | Influence of the Type of Water, Gas, and Plasma Sources on pH Value

Figure 15 reports the pH values of pure and tap water treated with multiple working gases and subjected to plasma jet, DBD, and corona discharge CAP sources (excluding gliding arc due to a lack of data, only 15 papers). Plasma jet treatments in pure water (Figure 15A) lead to lower median pH levels than tap water, regardless of the processed gas. Air leads to the highest acidification potential (median pH = 3), succeeded by argon (median pH = 3.9), helium (median pH = 4.2), and nitrogen (median pH = 5). The median pH related to plasma jet tap water treatments is higher than that of pure water, which is nearer to neutral levels. Indeed, all

16128869, 0, Downloaded from https://onlinelibrary.wiley.com/doi/10.1002/ppap.202400249 by Cochrane Slovakia, Wiley Online Library on [30/12/2024]. See the Terms and Conditions (https://onlinelibrary.wiley.com/terms-and-conditions) on Wiley Online Library for rules of use; OA articles are governed by the applicable Creative Commons License

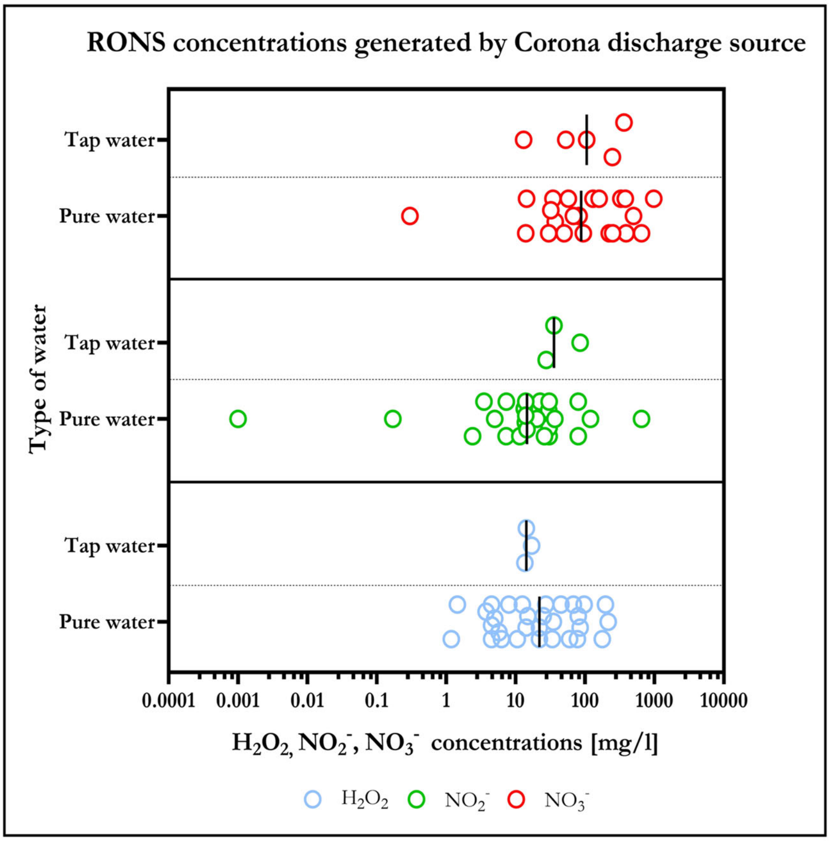

FIGURE 10 | Influence of the type of water on concentrations of RONS (H_2O_2, NO_2^-, NO_3^-), produced by corona discharge CAP source. The black line represents the median.

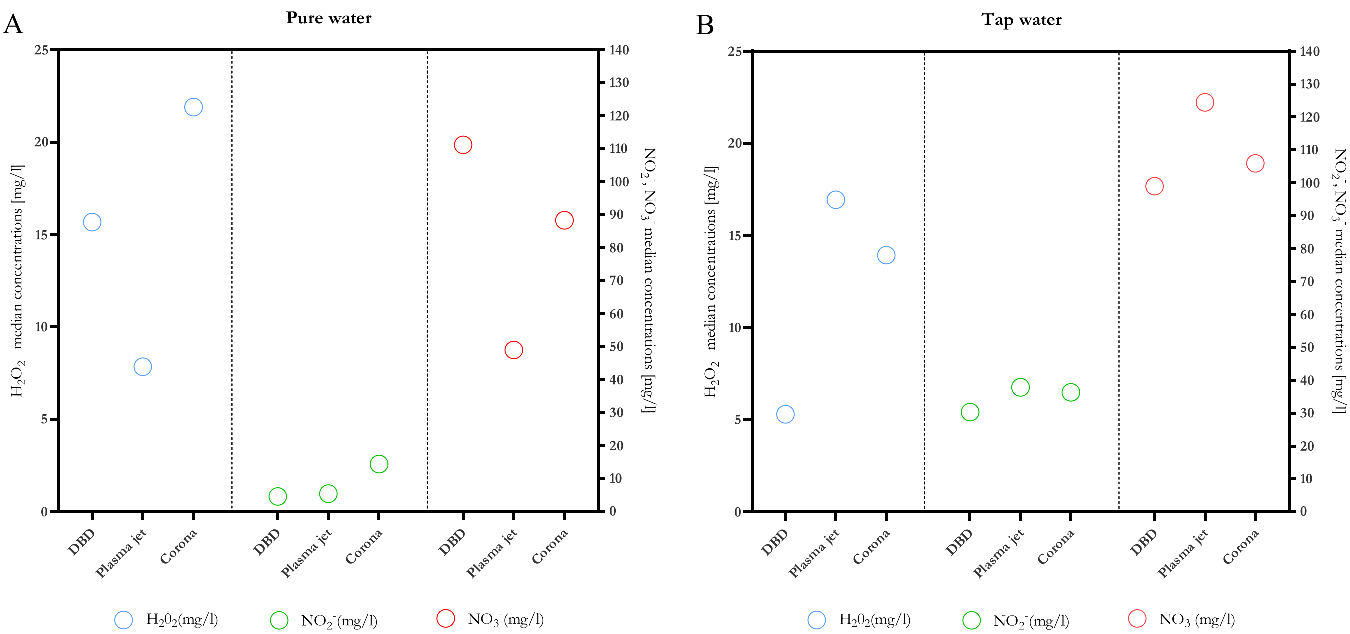

FIGURE 11 | Median value of concentrations of RONS (H_2O_2, NO_2^-, NO_3^-), produced by DBD, plasma jet, and corona discharge in pure (A) or tap (B) water.

median pH values fall within 6 and 7.5 when treating tap water due to weak carbonate buffering capacity in tap water. Figure 15B hinders a comprehensive assessment of the pH induced by DBD treatment of water. DBD generated in air induces higher pure and tap water acidification than air plasma jet treatments. Figure 15C shows pH values observed after pure and tap water corona discharge treatments. For pure water, air leads to the highest level of acidification, with a median pH of 3, indicating a strong acidic environment. Argon-treated water follows, with a median pH of 3.9, suggesting a slightly less acidic outcome. Helium and nitrogen PAW

16128869, 0, Downloaded from https://onlinelibrary.wiley.com/doi/10.1002/ppap.202400249 by Cochrane Slovakia, Wiley Online Library on [30/12/2024]. See the Terms and Conditions (https://onlinelibrary.wiley.com/terms-and-conditions) on Wiley Online Library for rules of use; OA articles are governed by the applicable Creative Commons License

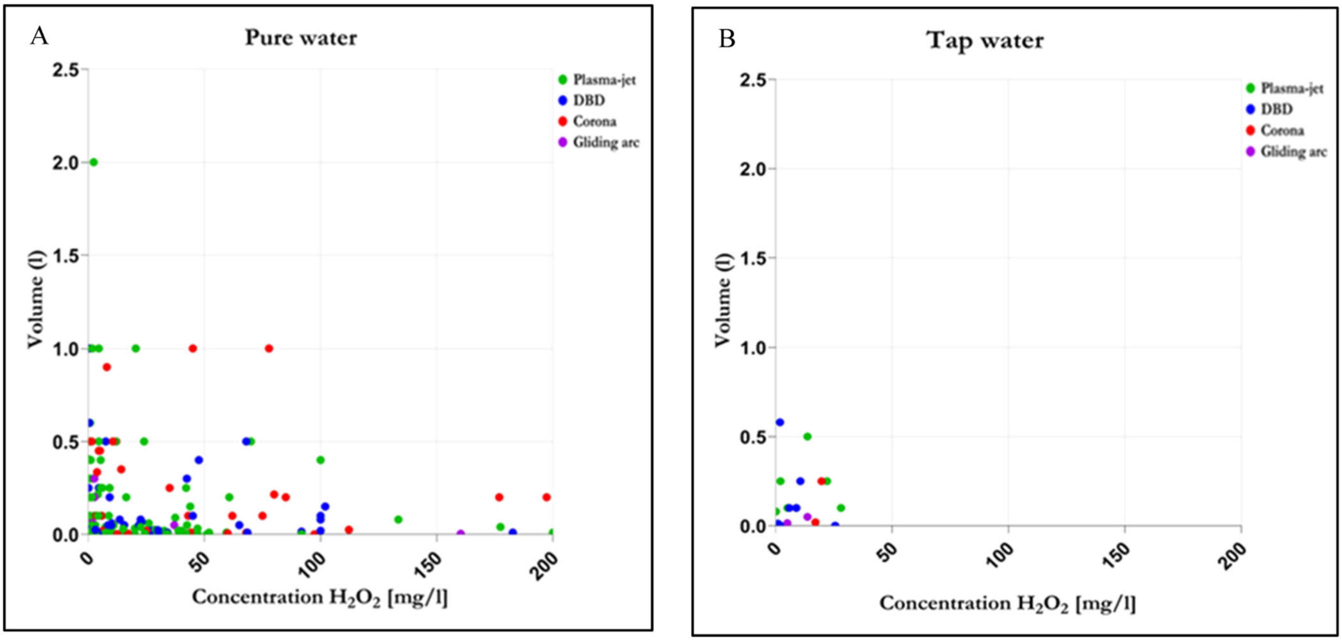

FIGURE 12 | Influence of treated volume and CAP source on H_2O_2 concentration in pure (A) and tap (B) water.

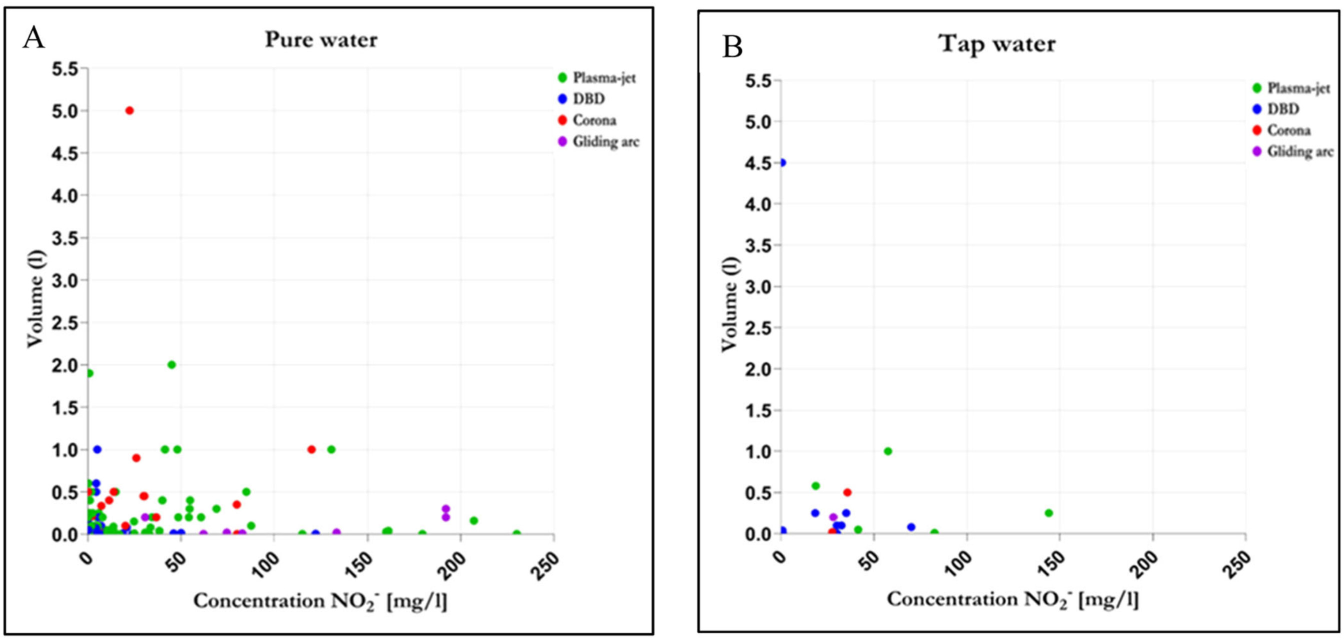

FIGURE 13 | Influence of treated volume and CAP source on NO_2^- concentration in pure (A) and tap (B) water.

treatment report median pH of 4.2 and 5, which is still acidic but less than the other gases mentioned. In contrast, treatments performed on tap water result in pH values that are closer to neutral values.

3.6 | Correlation Between Quantity and Concentrations of RONS Depending on CAP Source and Type of Water

Figures 16–18 show a comparative analysis of the quantities (mg) and concentrations (mg/L) of H_2O_2, NO_2^-, and NO_3^- measured after various plasma-water treatment methods. Each chart features two dashed lines representing the mean values of the reported parameters, dividing the plots into four quadrants.

Figure 16A presents the quantities of H_2O_2 in pure water. Data points from all CAP sources fall within the quadrant characterized by below-average values in both quantity and concentration. The highest H_2O_2 concentrations are equally found in the upper and bottom right quadrants, highlighting the highest quantities related to the highest reported concentrations. Notably, corona discharge and plasma jet treatments reveal the highest H_2O_2 quantities.

Figure 17A presents the quantities and concentrations of NO_2^-. Data points cluster in the quadrant denoted by below-average

16128869, 0, Downloaded from https://onlinelibrary.wiley.com/doi/10.1002/ppap.202400249 by Cochrane Slovakia, Wiley Online Library on [30/12/2024]. See the Terms and Conditions (https://onlinelibrary.wiley.com/terms-and-conditions) on Wiley Online Library for rules of use; OA articles are governed by the applicable Creative Commons License

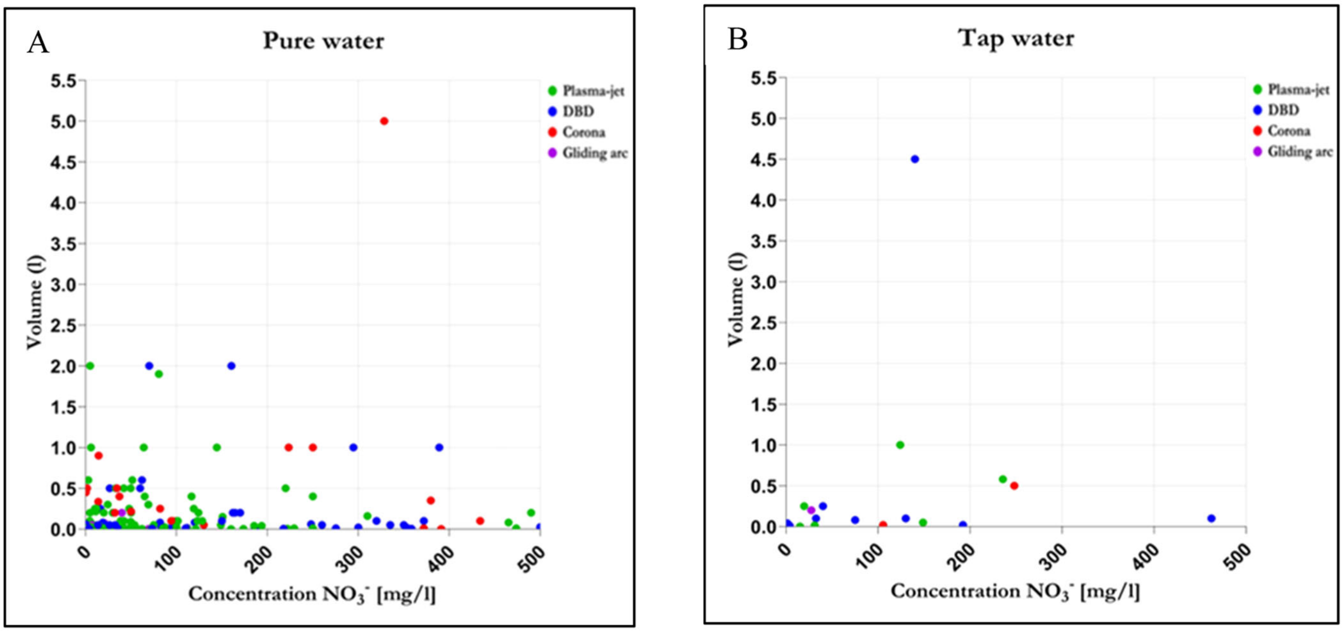

FIGURE 14 | Influence of treated volume and CAP source on NO_3^- concentration in pure (A) and tap (B) water.

values for quantity and concentration. The highest nitrite concentrations occur below the average quantities, although many cases are reported where above-average concentrations correspond to above-average quantities. Plasma jet treatments produce the highest NO_2^- quantities, while DBD treatments provide the lowest concentrations compared to the other CAP sources.

The analysis of NO_3^- quantities in pure water (Figure 18A) shows that the data set is mainly grouped below the average quantities, regardless of the CAP source. The highest NO_3^- concentrations are seldom observed above the mean quantity values. Plasma jet provides the highest NO_3^- quantities. Contrary to NO_2^- observations, the DBD is significantly represented in the fourth quadrant, emphasizing the production of above NO_3^- mean concentrations.

Figures 16B, 17B, and 18B depict the RONS quantities treating tap water. H_2O_2 quantities in tap water (Figure 16B) reveal a marked reduction in the mean production across all CAP sources compared to pure water treatment. The plasma jet shows a slight advantage in producing H_2O_2, although its mean production is reduced compared to pure water. The NO_2^- mean quantity in tap water (Figure 17B) is higher (9 mg) than in pure water treatment (5 mg). The plasma jet induces relatively higher NO_2^- concentrations than other sources, although its efficacy is lower than in pure water. Figure 18B illustrates the quantities and concentrations of NO_3^- in tap water. Despite the reduction in mean concentrations compared to pure water, the average quantity remains similar to that in pure water. Plasma jet and corona discharge produce the highest quantities of RONS.

3.7 | Correlation Between the Mean Energy Density and Concentration of RONS Depending on the Type of Plasma Source

Figures 19–21 present a detailed analysis of the mean energy density (kWh/L) delivered in the PAW production process using multiple CAP sources: plasma jet, DBD, corona, and gliding arc. Each scatter plot displays the concentration of H_2O_2, NO_2^- and NO_3^- versus the mean energy density, with performance boundaries for each source highlighted by dashed boxes.

Figure 19 displays the concentration of hydrogen peroxide against mean energy density. The DBD and plasma jet exhibit the broadest range of mean energy densities, but only the DBD reaches the highest concentrations. The corona discharge operates within a more limited density range and results in lower concentrations than DBD. The plasma jet and gliding arc require among the highest energy densities, even if the H_2O_2 concentrations are limited.

Figure 20 reports the concentration of nitrites versus the mean energy density. The DBD produces significant NO_2^- concentrations using a broad range of high energy density values. While capable of reaching high concentrations, the gliding arc and plasma jet reveal lower energy densities than the DBD. The plasma jet shows moderate mean energy values and is constrained within lower concentrations than DBD and gliding arc.

Figure 21 illustrates the concentrations of nitrates and mean energy density. The plasma jet and DBD provided the highest NO_3^- concentrations, but only DBD is associated with the highest mean energy density value. The plasma jets operate within a lower energy density range than the DBD but exhibit similar maximum concentrations. Corona discharge and gliding arc show lower concentrations than DBD and plasma jet, with lower mean energy density than DBD. These graphs highlight the varying efficiencies of plasma treatment methods in producing RONS in pure water. The DBD is the most versatile and capable of operating across a wide range of mean energy densities and can produce the highest concentration of hydrogen peroxides, nitrites, and nitrates. Although each treatment exhibits distinct average energy densities and RONS concentrations, they all share treated volumes characteristic of laboratory scales (below 0.5 L). The highest mean energy densities in each graph are

16128869, 0, Downloaded from https://onlinelibrary.wiley.com/doi/10.1002/ppap.202400249 by Cochrane Slovakia, Wiley Online Library on [30/12/2024]. See the Terms and Conditions (https://onlinelibrary.wiley.com/terms-and-conditions) on Wiley Online Library for rules of use; OA articles are governed by the applicable Creative Commons License

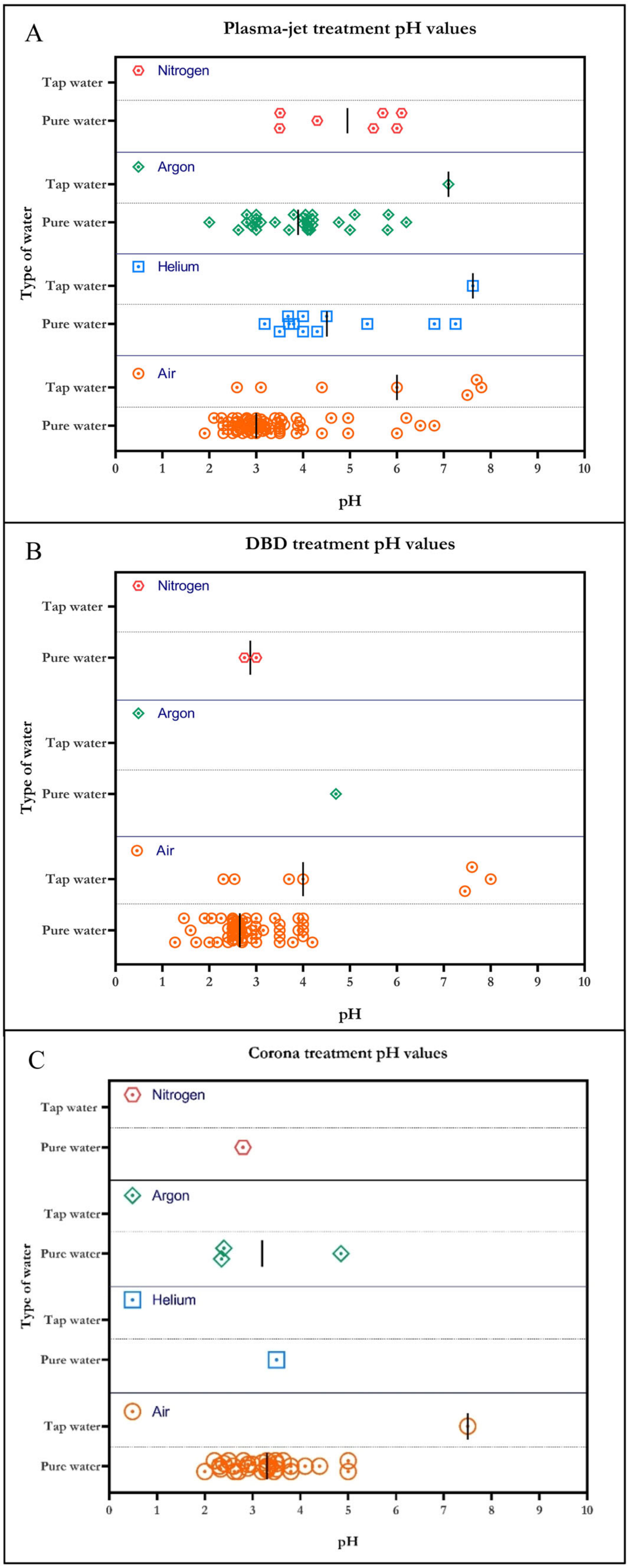

FIGURE 15 | Influence of type of water and working gas on pH value using plasma jet (A), DBD (B), and corona (C) source. The black line represents the median.

16128869, 0, Downloaded from https://onlinelibrary.wiley.com/doi/10.1002/ppap.202400249 by Cochrane Slovakia, Wiley Online Library on [30/12/2024]. See the Terms and Conditions (https://onlinelibrary.wiley.com/terms-and-conditions) on Wiley Online Library for rules of use; OA articles are governed by the applicable Creative Commons License

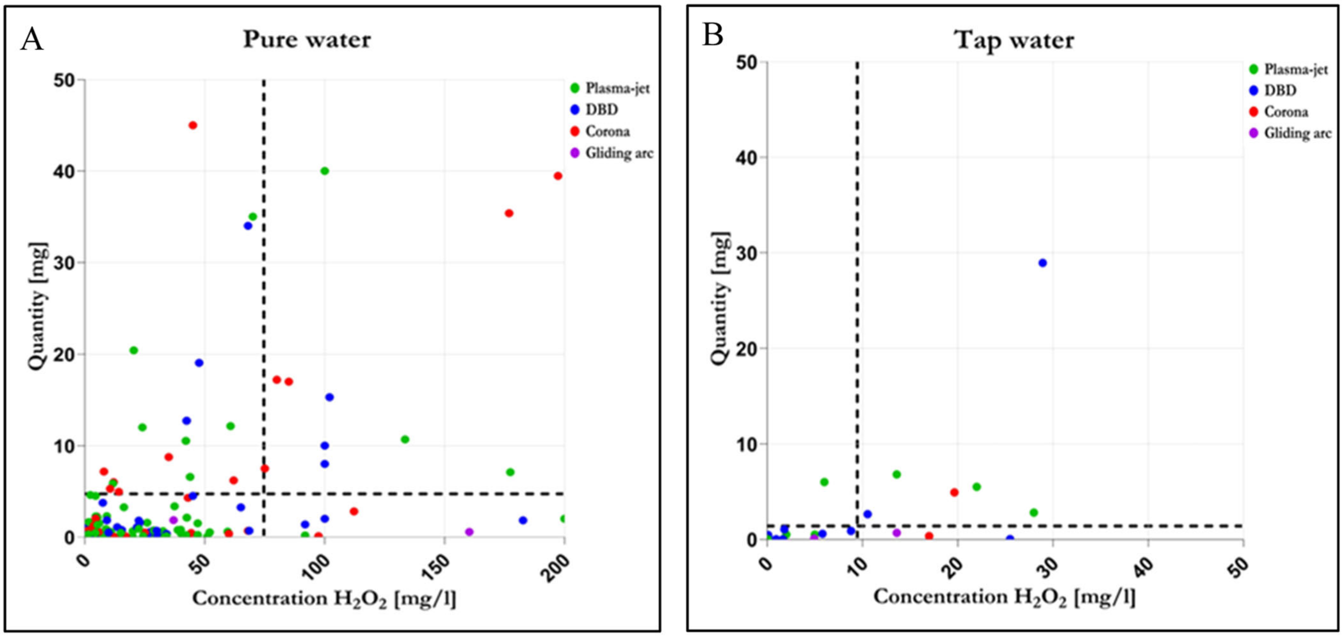

FIGURE 16 | Correlation between quantity and concentration of H_2O_2 in pure (A) and tap (B) water (right) depending on the type of CAP source. Dashed lines represent the mean values.

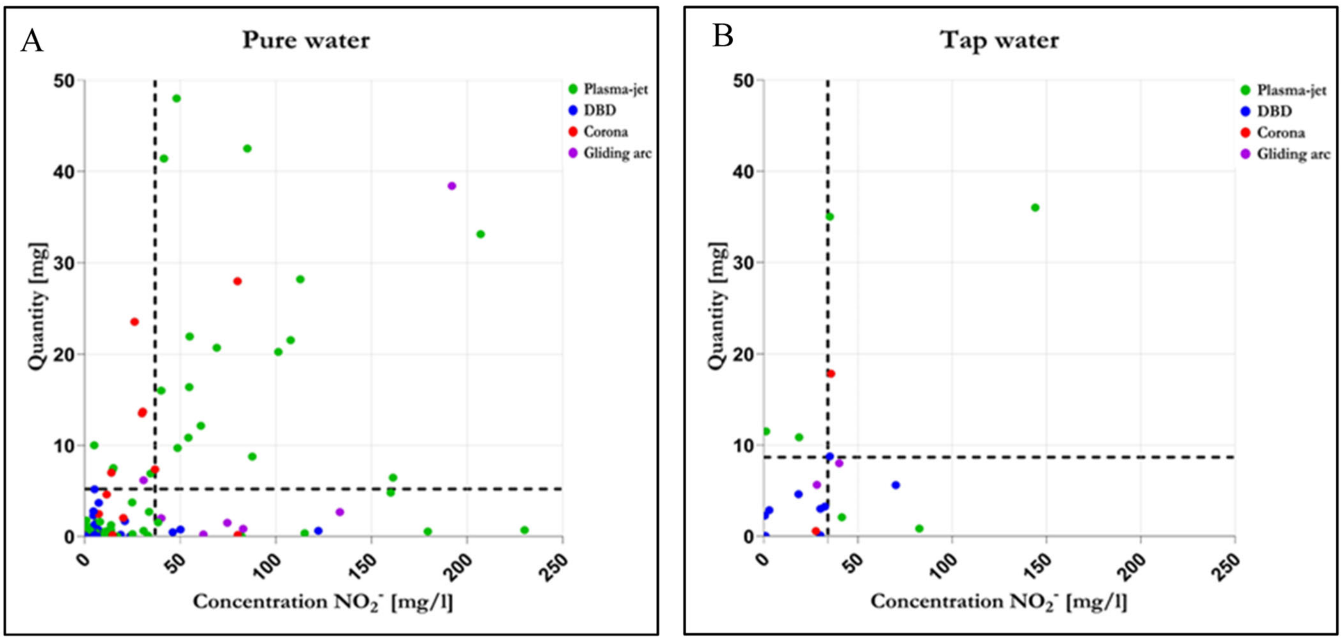

FIGURE 17 | Correlation between quantity and concentration of NO_2^- in pure (A) and tap (B) water, depending on the type of CAP source. Dashed lines represent the mean values.

related to Park et al. [57]. This article shows a PAW treatment based on a DBD source, treating 3 mL of distilled water for 10 min. The recorded discharge power is 61 W, and the final pH of the treated liquid is 3.5. The reported concentrations of H_2O_2, NO_2^- and NO_3^- are 34, 240, and 60 mg/L. Although this paper presents the highest mean energy density among those analyzed, it only corresponds to the highest concentrations in the case of nitrites. Rathore et al. [58] report the highest concentrations of hydrogen peroxides, with a DBD source employed to treat 20 mL of distilled water for 15 min at a discharge power of 30 W, inducing a hydrogen peroxide concentration of 103 mg/L. Finally, Miranda et al. [59] report the highest concentrations of nitrates. In this study, the PAW process utilized a DBD source to treat 25 mL of distilled water for 10 min, with a final nitrate concentration equal to 500 mg/L.

3.8 | Influence of Type of Water and Plasma Source on the Efficiency of RONS Production

Since the energy spent to generate plasma is used to produce various species, among which the long-lived ones are hydrogen peroxide, nitrites, and nitrates, an important parameter to

16128869, 0, Downloaded from https://onlinelibrary.wiley.com/doi/10.1002/ppap.202400249 by Cochrane Slovakia, Wiley Online Library on [30/12/2024]. See the Terms and Conditions (https://onlinelibrary.wiley.com/terms-and-conditions) on Wiley Online Library for rules of use; OA articles are governed by the applicable Creative Commons License

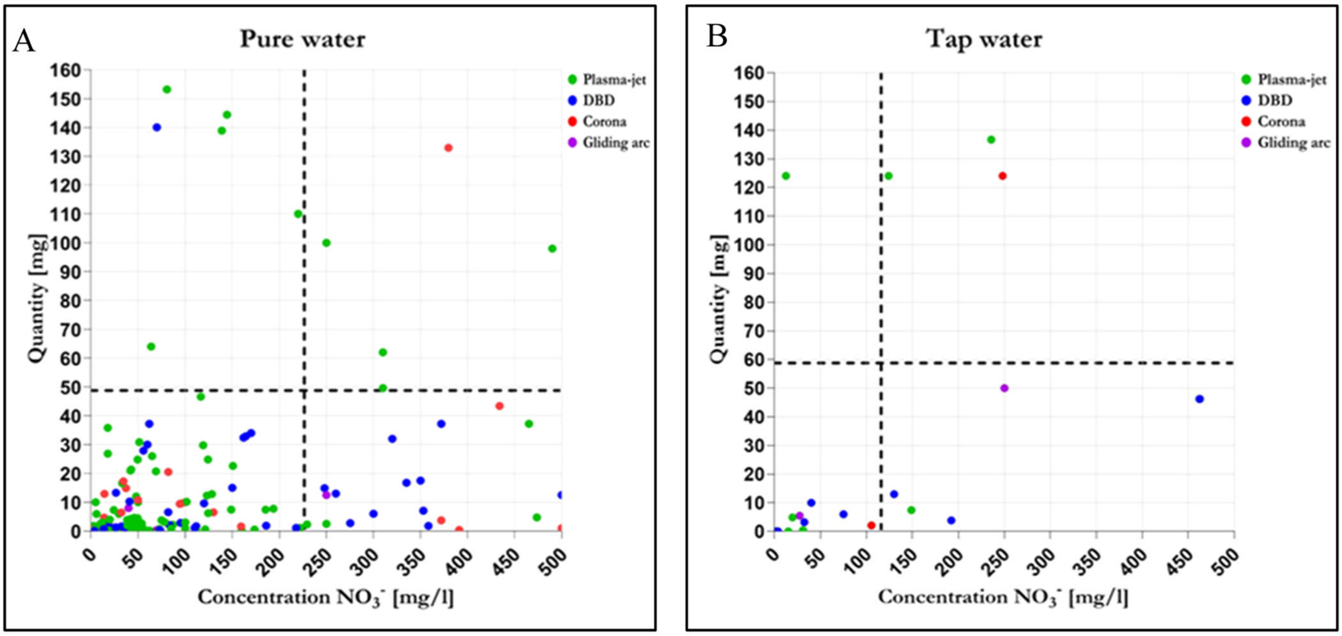

FIGURE 18 | Correlation between quantity and concentration of NO_3^- in pure (A) and tap (B) water, depending on the type of CAP source. Dashed lines represent the mean values.

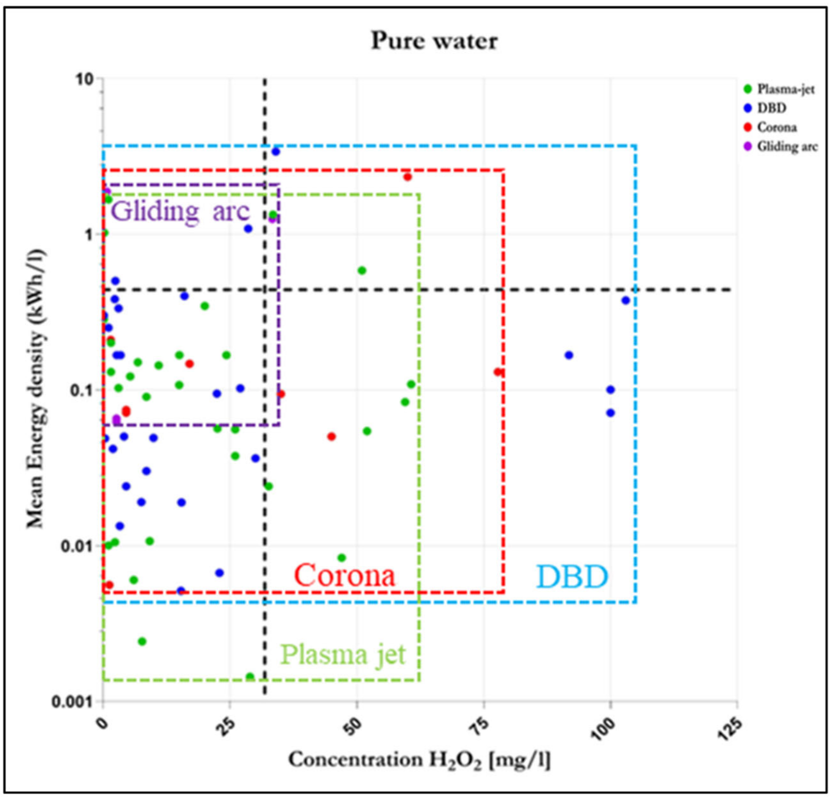

FIGURE 19 | Correlation between mean energy density and concentration of H_2O_2 in pure water, depending on the type of plasma source. Black dashed lines represent the mean values.

compare the processes, especially for potential industrial scale-up, is the efficiency of RONS production. This parameter has been calculated by dividing the molar amounts of hydrogen peroxide, nitrites, and nitrates by the energy consumption. Figure 22 illustrates the efficiency of RONS production in pure and tap water. Figure 22A reports the efficiency of RONS production in pure water, covering a broader range of efficiency values than tap water. The highest efficiencies result close to 1 mol/kWh, and are related to the studies of Xu [60] using a plasma jet for the treatment of 3 mL of pure water, and Bălan [61], where 300 mL of distilled water are exposed to a gliding arc for 10 min. However, many studies report much lower

16128869, 0, Downloaded from https://onlinelibrary.wiley.com/doi/10.1002/ppap.202400249 by Cochrane Slovakia, Wiley Online Library on [30/12/2024]. See the Terms and Conditions (https://onlinelibrary.wiley.com/terms-and-conditions) on Wiley Online Library for rules of use; OA articles are governed by the applicable Creative Commons License

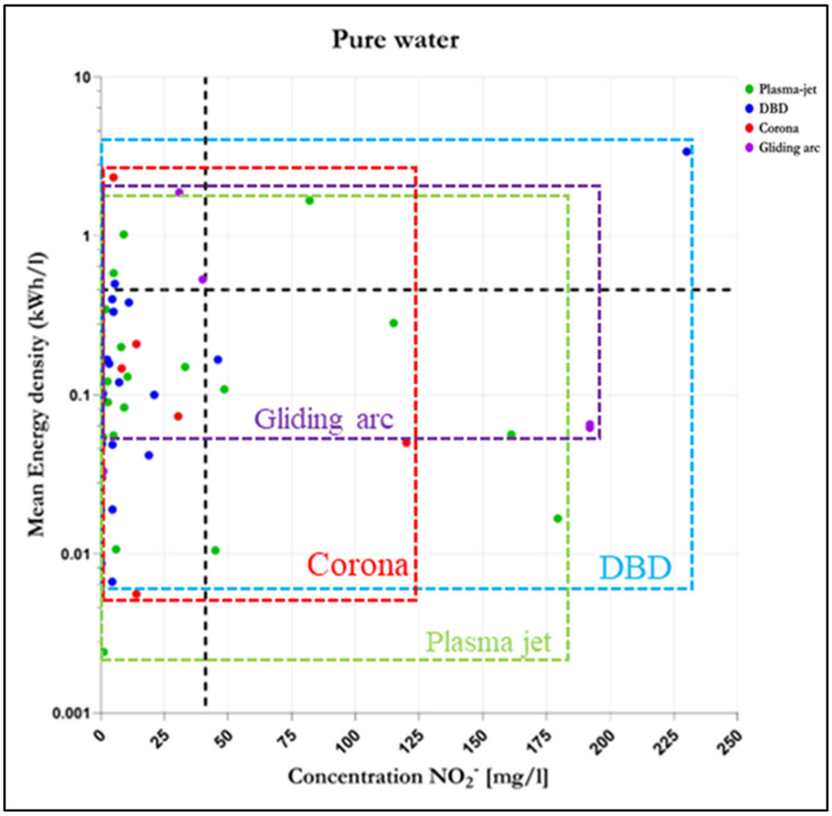

FIGURE 20 | Correlation between mean energy density and concentration of NO_2^- in pure water, depending on the type of plasma source. Black dashed lines represent the mean values.

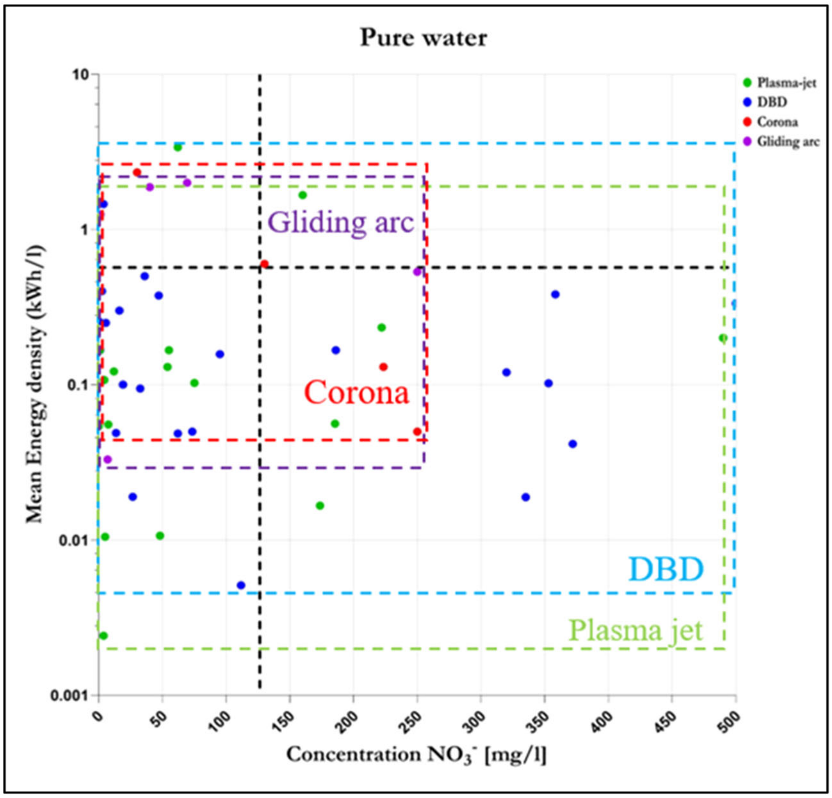

FIGURE 21 | Correlation between mean energy density and concentration of NO_3^- in pure water, depending on the type of plasma source. Dashed lines represent the mean values.

16128869, 0, Downloaded from https://onlinelibrary.wiley.com/doi/10.1002/ppap.202400249 by Cochrane Slovakia, Wiley Online Library on [30/12/2024]. See the Terms and Conditions (https://onlinelibrary.wiley.com/terms-and-conditions) on Wiley Online Library for rules of use; OA articles are governed by the applicable Creative Commons License

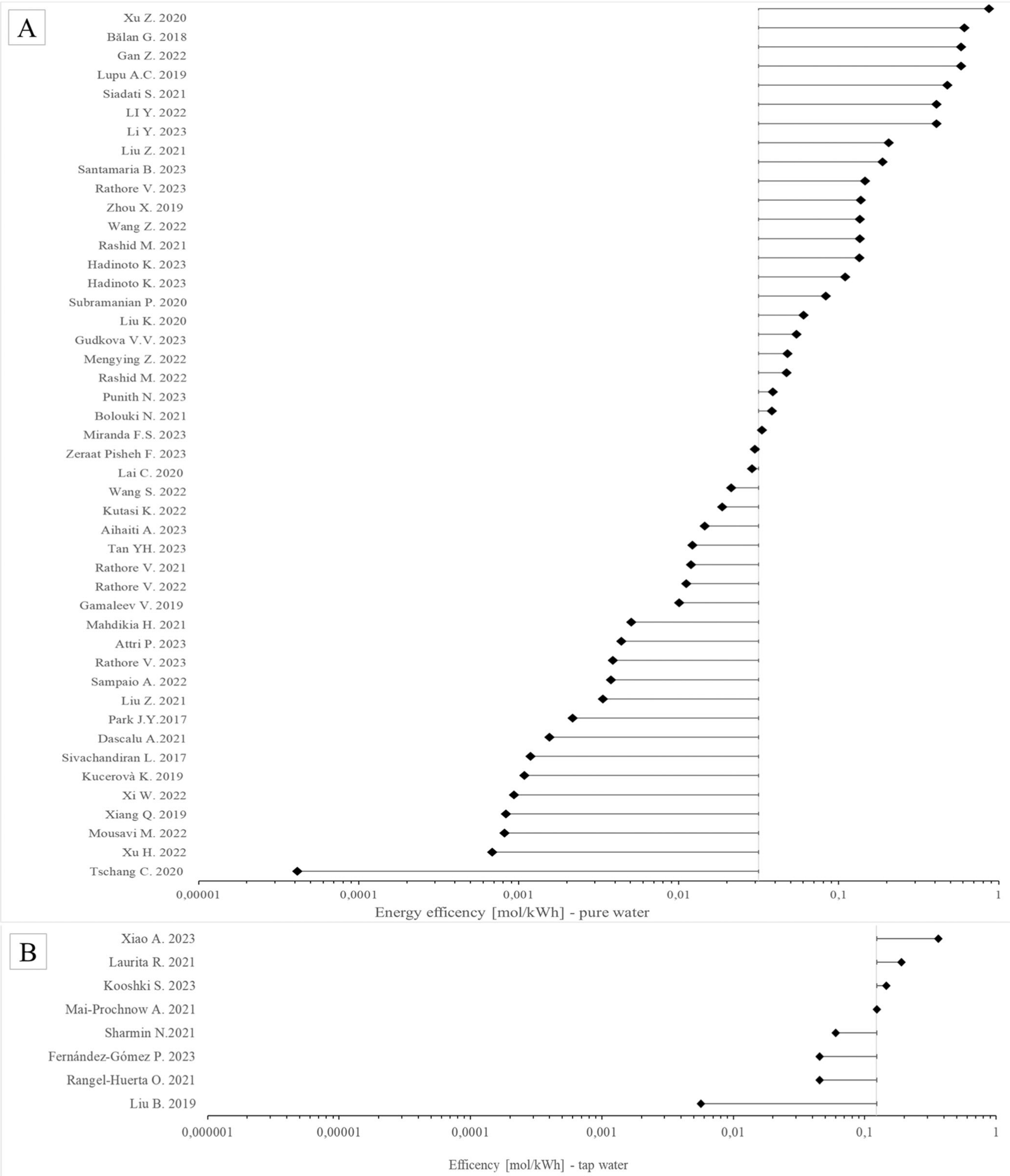

FIGURE 22 | Efficiency of RONS production in pure (A) and tap (B) water. The vertical line represents the median.

efficiencies, clustering around 0.01–0.1 mol/kWh. Figure 22B focuses on RONS production efficiency in tap water; the efficiency values vary significantly among the studies, spanning from approximately 0.001 to 1 mol/kWh. Notably, the study by Xiao et al. [62] reports a DBD treatment of 1 l of tap water for 1 h, resulting in the highest efficiency among the analyzed paper dealing with plasma treatments of TAP water, about 1 mol/kWh. Figure 22 reveals that the efficiency of RONS production in pure water tends to be higher than in tap water. The top-performing studies in both water types achieve similar maximum efficiencies, indicating that high RONS production efficiency is achievable in both water media with optimized conditions.

16128869, 0, Downloaded from https://onlinelibrary.wiley.com/doi/10.1002/ppap.202400249 by Cochrane Slovakia, Wiley Online Library on [30/12/2024]. See the Terms and Conditions (https://onlinelibrary.wiley.com/terms-and-conditions) on Wiley Online Library for rules of use; OA articles are governed by the applicable Creative Commons License

4 | Conclusions

This systematic review highlights the various methodologies evidenced within the PAW production reported in 358 original studies from 2017 to 2023. The presented study systematically correlates the plasma-water process parameters with the pH levels and RONS concentrations in PAW and reports results concerning the average energy density and the efficiency of RONS production.

Examining multiple CAP sources, particularly the plasma jets, DBDs, and corona discharges, underlines their distinct influences on RONS production. Figures 16–18 demonstrate that the plasma jet produces among the highest average quantities of RONS in pure and tap water, although the treated volumes are predominantly on a laboratory scale. Our findings suggest that despite specific methods permitting high RONS concentrations, the overall efficiency of RONS production is generally low, with most values reported by the studies below 0.1 mol/kWh, as demonstrated in Figure 22. A critical remark concerns the energy densities. It is worth noting that the heat capacity of water is 4182 J/kg·K; thus, processes in which the average energy density exceeds 334.6 J/mL, i.e., 0.093 kWh/L, if entirely transferred to the water, can cause an increase of ~80 K in the water temperature, leading to its boiling. This must be considered in the analysis of industrial development of PAW production processes. In addition, it should be considered that efficiency does not reflect the actual plant costs, as auxiliary systems for control or cooling of the sources may be necessary when working with large-scale plants. Particularly in the context of scaling up processes, a comprehensive assessment of both capital (mainly related to high power supplies) and operational costs will need to be considered in order to make plasma-assisted liquid production feasible for industrial processes.

Despite significant challenges in improving the efficiency of PAW production, which is essential for its practical applications, the potential of PAW remains considerable. Specific treatments have demonstrated high RONS production rates, indicating that more efficient PAW production methods can be developed with targeted research and optimization. This review advances our understanding of PAW processes and mechanisms and sets the groundwork for future research to improve RONS production efficiency. By identifying key factors that influence the efficacy of PAW, our work provides a valuable framework for comparing future PAW production systems with the literature-reported ones.

Acknowledgments

The authors thank the COST Action PlAgri, CA19110, supported by COST (European Cooperation in Science and Technology). This work was funded by the EU NextGenerationEU through the Recovery and Resilience Plan for Slovakia under Project No. 09I03-03-V03-00033 EnvAdwice. This work was funded by the EU NextGenerationEU through the Recovery and Resilience Plan for Italy under the project "PAAFOOD Plasma activated aerosol for the preservation and decontamination of fresh and minimally processed plant foods", No. 2022W43KHF_002 – CUP J53D23010480001. Open access publishing facilitated by Universita degli Studi di Bologna, as part of the Wiley - CRUI-CARE agreement.

Data Availability Statement

The data that support the findings of this study are openly available in AMSacta at https://doi.org/10.6092/unibo%2Famsacta%2F7933.

References

1. C. Bradu, K. Kutasi, M. Magureanu, N. Puač, and S. Živković, "Reactive Nitrogen Species in Plasma-Activated Water: Generation, Chemistry and Application in Agriculture," *Journal of Physics D: Applied Physics* 53 (2020): 223001.

2. X. Lu, G. V. Naidis, M. Laroussi, S. Reuter, D. B. Graves, and K. Ostrikov, "Reactive Species in Non-Equilibrium Atmospheric-Pressure Plasmas: Generation, Transport, and Biological Effects," 630 (2016): 1–84.

3. S. Mohades, A. M. Lietz, and M. J. Kushner, "Generation of Reactive Species in Water Film Dielectric Barrier Discharges Sustained in Argon, Helium, Air, Oxygen and Nitrogen," *Journal of Physics D: Applied Physics* 53 (2020): 435206.

4. F. Girard, V. Badets, S. Blanc, et al., "Formation of Reactive Nitrogen Species Including Peroxynitrite in Physiological Buffer Exposed to Cold Atmospheric Plasma," *RSC Advances* 6 (2016): 78457–78467.

5. G. Uchida, A. Nakajima, T. Ito, et al., "Effects of Nonthermal Plasma Jet Irradiation on the Selective Production of H_2O_2 and NO_2- in Liquid Water," *Journal of Applied Physics* 120 (2016): 20.

6. O. Kostya, R. Zhou, R. Zhou, et al., "Plasma-Activated Water: Generation, Origin of Reactive Species and Biological Applications," *Journal of Physics D: Applied Physics* 53 (2020): 303001.

7. J. L. Brisset and J. Pawlat, "Chemical Effects of Air Plasma Species on Aqueous Solutes in Direct and Delayed Exposure Modes: Discharge, Post-Discharge and Plasma Activated Water," *Plasma Chemistry and Plasma Processing* 36 (2016): 355–381.

8. X. Zhang, R. Zhou, K. Bazaka, et al., "Quantification of Plasma Produced OH Radical Density for Water Sterilization," *Plasma Processes and Polymers* 15 (2018): 6.

9. W. F. L. M. Hoeben, P. P. van Ooij, D. C. Schram, T. Huiskamp, A. J. M. Pemen, and P. Lukeš, "On the Possibilities of Straightforward Characterization of Plasma Activated Water," *Plasma Chemistry and Plasma Processing* 39 (2019): 597–626.

10. P. Heirman, W. Van Boxem, and A. Bogaerts, "Reactivity and Stability of Plasma-Generated Oxygen and Nitrogen Species in Buffered Water Solution: A Computational Study," *Physical Chemistry Chemical Physics* 21 (2019): 12881–12894.

11. J. Shen, H. Zhang, Z. Xu, et al., "Preferential Production of Reactive Species and Bactericidal Efficacy of Gas-Liquid Plasma Discharge," *Chemical Engineering Journal* 362 (2019): 402–412.

12. K. Takahashi, K. Satoh, H. Itoh, et al., "Production Characteristics of Reactive Oxygen/Nitrogen Species in Water Using Atmospheric Pressure Discharge Plasmas," *Japanese Journal of Applied Physics* 55 (2016): 7S2.

13. Z. Machala, B. Tarabová, D. Sersenová, M. Janda, and K. Hensel, "Chemical and Antibacterial Effects of Plasma Activated Water: Correlation With Gaseous and Aqueous Reactive Oxygen and Nitrogen Species, Plasma Sources and Air Flow Conditions," *Journal of Physics D: Applied Physics* 52 (2019): 034002.

14. C. Y. Hou, Y. C. Lai, C. P. Hsiao, et al., "Antibacterial Activity and the Physicochemical Characteristics of Plasma Activated Water on Tomato Surfaces," *LWT* 149 (2021): 111879.

15. S. Mitra, M. Veerana, E. H. Choi, and G. Park, "Effects of Pre-Treatment Using Plasma on the Antibacterial Activity of Mushroom Surfaces," *Foods* 10 (2021): 1888.

16. Q. Xiang, C. Kang, L. Niu, D. Zhao, K. Li, and Y. Bai, "Antibacterial Activity and a Membrane Damage Mechanism of Plasma-Activated Water Against *Pseudomonas deceptionensis* CM2," *LWT* 96 (2018): 395–401.

17. M. Ali, J. H. Cheng, and D. W. Sun, "Combined Application of Ascorbic and Oxalic Acids Delays Postharvest Browning of Litchi Fruits

16128869, 0, Downloaded from https://onlinelibrary.wiley.com/doi/10.1002/ppap.202400249 by Cochrane Slovakia, Wiley Online Library on [30/12/2024]. See the Terms and Conditions (https://onlinelibrary.wiley.com/terms-and-conditions) on Wiley Online Library for rules of use; OA articles are governed by the applicable Creative Commons License

Under Controlled Atmosphere Conditions," *Food Chemistry* 350 (2021): 129277.

18. D. Yan, J. H. Sherman, and M. Keidar, "Cold Atmospheric Plasma, a Novel Promising Anti-Cancer Treatment Modality," *Oncotarget* 8 (2017): 15977–15995.

19. B. Pang, Z. Liu, S. Wang, et al., "Discharge Mode Transition in a He/Ar Atmospheric Pressure Plasma Jet and Its Inactivation Effect Against Tumor Cells In Vitro," *Journal of Applied Physics* 130 (2021): 15.

20. L. Gan, J. Jiang, J. W. Duan, et al., "Cold Atmospheric Plasma Applications in Dermatology: A Systematic Review," *Journal of Biophotonics* 14 (2021): e202000415.

21. Z. Liu, Y. Zheng, J. Dang, et al., "A Novel Antifungal Plasma-Activated Hydrogel," *ACS Applied Materials & Interfaces* 11 (2019): 22941–22949.

22. Y. Li, M. H. Kang, H. S. Uhm, G. J. Lee, E. H. Choi, and I. Han, "Effects of Atmospheric-Pressure Non-Thermal Bio-Compatible Plasma and Plasma Activated Nitric Oxide Water on Cervical Cancer Cells," *Scientific Reports* 31 (2017): 7.

23. A. Vaid, C. Patil, A. Sanghariyat, et al., "Emerging Advanced Technologies Developed by IPR for Bio Medical Applications—A Review," *Neurology India* 68 (2020): 26–34.

24. D. Boehm, J. Curtin, P. J. Cullen, and P. Bourke, "Hydrogen Peroxide and Beyond-the Potential of High-Voltage Plasma-Activated Liquids Against Cancerous Cells," *Anti-Cancer Agents in Medicinal Chemistry* 18 (2018): 815–823.

25. S. Raud, J. Raud, I. Jõgi, et al., "The Production of Plasma Activated Water in Controlled Ambient Gases and Its Impact on Cancer Cell Viability," *Plasma Chemistry and Plasma Processing* 41 (2021): 1381–1395.

26. A. Bisag, P. Isabelli, R. Laurita, et al., "Cold Atmospheric Plasma Inactivation of Aerosolized Microdroplets Containing Bacteria and Purified SARS-CoV-2 RNA to Contrast Airborne Indoor Transmission," *Plasma Processes and Polymers* 17 (2020): 2000154.

27. A. Bisag, P. Isabelli, G. Laghi, et al., "Cold Atmospheric Plasma Decontamination of SARS-CoV-2 Bioaerosols," *Plasma Processes and Polymers* 19 (2022): e2100133.

28. N. Puač, M. Gherardi, and M. Shiratani, "Plasma Agriculture: A Rapidly Emerging Field," *Plasma Processes and Polymers* 15 (2018): 2.

29. F. Judée, S. Simon, C. Bailly, and T. Dufour, "Plasma-Activation of Tap Water Using DBD for Agronomy Applications: Identification and Quantification of Long Lifetime Chemical Species and Production/Consumption Mechanisms," *Water Research* 133 (2018): 47–59.

30. K. Kučerová, M. Henselová, Ľ. Slováková, and K. Hensel, "Effects of Plasma Activated Water on Wheat: Germination, Growth Parameters, Photosynthetic Pigments, Soluble Protein Content, and Antioxidant Enzymes Activity," *Plasma Processes and Polymers* 16 (2019): 1800131.

31. M. Bafoil, A. Jemmat, Y. Martinez, et al., "Effects of Low Temperature Plasmas and Plasma Activated Waters on *Arabidopsis thaliana* Germination and Growth," *PLoS One* 13 (2018): e0195512.

32. L. Sivachandiran and A. Khacef, "Enhanced Seed Germination and Plant Growth by Atmospheric Pressure Cold Air Plasma: Combined Effect of Seed and Water Treatment," *RSC Advances* 7 (2017): 1822–1832.

33. Y. Tanakaran, V. Luang-In, and K. Matra, "Effect of Atmospheric Pressure Multicorona Air Plasma and Plasma-Activated Water on Germination and Growth of Rat-Tailed Radish Seeds," *IEEE Transactions on Plasma Science* 49 (2021): 563–572.

34. C. Alves, F. De Menezes, J. De, and O. Vitoriano, "Effect of Plasma-Activated Water on Soaking, Germination, and Vigor of Erythrina Velutina Seeds," *Plasma Medicine* 9 (2019): 111–120.

35. S. Z. Ismail, M. M. Khandaker, N. Mat, and A. N. Boyce, "Effects of Hydrogen Peroxide on Growth, Development and Quality of Fruits: A Review," *Journal of Agronomy* 14 (2015): 331–336.

36. P. Dimitrakellis, M. Giannoglou, Z. M. Xanthou, E. Gogolides, P. Taoukis, and G. Katsaros, "Application of Plasma-Activated Water as an Antimicrobial Washing Agent of Fresh Leafy Produce," *Plasma Processes and Polymers* 18 (2021): 2100030.

37. R. Dhivya, V. C. Rajakrishnapriya, K. Sruthi, D. V. Chidanand, C. K. Sunil, and A. Rawson, "Biofilm Combating in the Food Industry: Overview, Non-Thermal Approaches, and Mechanisms," *Journal of Food Processing and Preservation* 46 (2022): 10.

38. C. Sarangapani, L. Scally, M. Gulan, and P. J. Cullen, "Dissipation of Pesticide Residues on Grapes and Strawberries Using Plasma-Activated Water," *Food and Bioprocess Technology* 13 (2020): 1728–1741.

39. J. Qian, H. Zhuang, M. M. Nasiru, U. Muhammad, and J. Zhang, "W. Yan. "Action of Plasma-Activated Lactic Acid on the Inactivation of Inoculated Salmonella Enteritidis and Quality of Beef," *Innovative Food Science and Emerging Technologies* 1 (2019): 57.

40. R. Zhou, R. Zhou, A. Mai-Prochnow, et al., "Surface Plasma Discharges for the Preservation of Fresh-Cut Apples: Microbial Inactivation and Quality Attributes," *Journal Physics D: Applied Physics* 53 (2020): 17.

41. R. Laurita, G. Gozzi, S. Tappi, et al., "Effect of Plasma Activated Water (PAW) on Rocket Leaves Decontamination and Nutritional Value," *Innovative Food Science and Emerging Technologies* 73 (2021): 102805.

42. J. Barrales Astorga, K. Hadinoto, P. Cullen, S. Prescott, and F. J. Trujillo, "Effect of Plasma Activated Water on the Nutritional Composition, Storage Quality and Microbial Safety of Beef," *LWT* 154 (2022): 112794.

43. F. Capelli, S. Tappi, T. Gritti, et al. "Decontamination of Food Packages From SARS-COV-2 RNA With a Cold Plasma-Assisted System," *Applied Sciences* 1 (2021): 9.

44. M. R. Webb and G. M. Hieftje, "Spectrochemical Analysis by Using Discharge Devices With Solution Electrodes," *Analytical Chemistry* 81 (2009): 862–867.

45. M. Smoluch, P. Mielczarek, and J. Silberring, "Plasma-Based Ambient Ionization Mass Spectrometry in Bioanalytical Sciences," *Mass Spectrometry Reviews* 35 (2016): 22–34.

46. A. T. Ambujakshan, J. M. Pringle, Z. Chen, et al., "An Environmentally Friendly In Situ Plasma and Anodization Method to Produce Titanium Dioxide Nanotubes," *Plasma Processes and Polymers* 1 (2018): 15.

47. G. Laghi, D. Franco, G. G. Condorelli, et al., "Control Strategies for Atmospheric Pressure Plasma Polymerization of Fluorinated Silane Thin Films With Antiadhesive Properties," *Plasma Processes and Polymers* 20 (2023): 2200194.

48. U. Cvelbar, J. L. Walsh, M. Černák, et al., "White Paper on the Future of Plasma Science and Technology in Plastics and Textiles," *Plasma Processes and Polymers* 16 (2019): 1.

49. H. Malekzad, T. Gallingani, F. Barletta, et al. "Single-Step Deposition of Hexamethyldisiloxane Surface Gradient Coatings With a High Amplitude of Water Contact Angles Over a Polyethylene Foil," *Plasma Processes and Polymers* 1 (2021): 2.

50. M. J. Page, J. E. McKenzie, P. M. Bossuyt, et al., "The PRISMA 2020 Statement: An Updated Guideline for Reporting Systematic Reviews," *British Medical Journal* 372 (2021): 71.

51. B. Surowsky, O. Schlüter, and D. Knorr, "Interactions of Non-Thermal Atmospheric Pressure Plasma With Solid and Liquid Food Systems: A Review," *Food Engineering Reviews* 7 (2015): 82–108.

52. K. Kučerová, Z. Machala, and K. Hensel, "Transient Spark Discharge Generated in Various N_2/O_2 Gas Mixtures: Reactive Species in

16128869, 0, Downloaded from https://onlinelibrary.wiley.com/doi/10.1002/ppap.202400249 by Cochrane Slovakia, Wiley Online Library on [30/12/2024]. See the Terms and Conditions (https://onlinelibrary.wiley.com/terms-and-conditions) on Wiley Online Library for rules of use; OA articles are governed by the applicable Creative Commons License

the Gas and Water and Their Antibacterial Effects," *Plasma Chemistry and Plasma Processing* 40 (2020): 749–773.

53. F. G. Chizoba Ekezie, D. W. Sun, and J. H. Cheng, "A Review on Recent Advances in Cold Plasma Technology for the Food Industry: Current Applications and Future Trends," *Trends in Food Science & Technology* 69 (2017): 46–58.

54. P. Starič, K. Vogel-Mikuš, M. Mozetič, and I. Junkar, "Effects of Nonthermal Plasma on Morphology, Genetics and Physiology of Seeds: A Review," *Plants* 9 (2020): 1736.

55. K. Adesina, T. C. Lin, Y. W. Huang, M. Locmelis, and D. Han, "A Review of Dielectric Barrier Discharge Cold Atmospheric Plasma for Surface Sterilization and Decontamination," *IEEE Transactions on Radiation and Plasma Medical Sciences* 8 (2024): 295–306.

56. J. Pawłat, P. Terebun, M. Kwiatkowski, et al., "Evaluation of Oxidative Species in Gaseous and Liquid Phase Generated by Mini-Gliding Arc Discharge," *Plasma Chemistry and Plasma Processing* 39 (2019): 627–642.

57. J. Y. Park, S. Park, W. Choe, H. I. Yong, C. Jo, and K. Kim, "Plasma-Functionalized Solution: A Potent Antimicrobial Agent for Biomedical Applications From Antibacterial Therapeutics to Biomaterial Surface Engineering," *ACS Applied Materials & Interfaces* 9 (2017): 43470–43477.

58. V. Rathore, C. Patil, and A. Sanghariyat, "S. K. Nema. "Design and Development of Dielectric Barrier Discharge Setup to Form Plasma-Activated Water and Optimization of Process Parameters," *European Physical Journal D* 76 (2022): 5.

59. F. S. Miranda, V. K. F. vares, M. P. Gomes, et al., "Physicochemical Characteristics and Antimicrobial Efficacy of Plasma-Activated Water Produced by an Air-Operated Coaxial Dielectric Barrier Discharge Plasma," *Water* 15 (2023): 23.

60. Z. Xu, X. Zhou, W. Yang, et al., *Plasma Processes and Polymers* 17 (2020): 8.

61. G. G. Bălan, I. Roşca, E. L. Ursu, et al., "Plasma-Activated Water: A New and Effective Alternative for Duodenoscope Reprocessing," *Infection and Drug Resistance* 11 (2018): 727–733.

62. A. Xiao, D. Liu, and Y. Li, "Plasma-Activated Tap Water Production and Its Application Inatomization Disinfection," *Applied Science* 13 (2023): 3015.

16128869, 0, Downloaded from https://onlinelibrary.wiley.com/doi/10.1002/ppap.202400249 by Cochrane Slovakia, Wiley Online Library on [30/12/2024]. See the Terms and Conditions (https://onlinelibrary.wiley.com/terms-and-conditions) on Wiley Online Library for rules of use; OA articles are governed by the applicable Creative Commons License